CHARACTERIZATION OF NONDIFFRACTING BESSEL BEAMS IN THE PROPAGATION RANGE

S.A. AMARANDE

National Institute for Laser, Plasma and Radiation Physics, Laser Section, P.O. Box MG-36, RO-077125 Bucharest-Magurele, Romania, E-mail: stefan.amarande@inflpr.ro

Abstract. Nondiffractive Bessel beams were generated experimentally and their propagation was characterized using the self-convergent width method. By the use of this criterion for the calculation of the truncated second-moment of the irradiance, the invariant propagation of the generated Bessel beams is confirmed.

Key words: nondiffractive/propagation invariant beams, Bessel beams, self-convergent beam width.

1. INTRODUCTION

Nondiffracting beams are propagation-invariant sharply peaked solutions of the scalar wave equation [1, 2]. These beams can be understood intuitively as a set of plane waves whose wave vectors lie on a cone around propagation axis. As the phase between these plane waves does not change in propagation, their interference pattern is the same at any plane z. The simplest beam of this kind is the Bessel beam. This beam has circular symmetry and a transverse distribution with the form of a Bessel function of first kind and zero order, $J_0(k_r r)$, where r is the distance from z axis and k_r is the length of the component, orthogonal to the propagation axis, of any wave vector belonging to one of the interfering plane waves. Although these beams have strictly infinite extent and energy, their finite-aperture approximations [3] and experimental counterparts [1] have diffraction-free propagation over long distances. In fact, strictly speaking, real nondiffracting Bessel beams have an irradiance distribution that is propagation invariant but not strictly diffraction free [4]. However, the J_0 solution of wave equation describes the propagation of a narrow beam (namely the central portion of the J_0^2 transverse-irradiance distribution) without spreading over much longer distances as the Rayleigh range of equivalent (with the same initial full width at half maximum) Gaussian beams. Due to this peculiar property, Bessel beams have been used in applications such as microscopy [5], micromanipulation [6], material processing

[7] and free-space optical communications [8]. For these applications, the useful part of the Bessel beams is often limited to their near field. As a matter of fact, the central lobe persists as long as there are off-axis lobes to replenish its diffraction losses and prevent it from spreading [9, 10]. It is also this replenishment that allows Bessel beam to reconstruct itself if blocked [10, 11]. Experimental investigations of Bessel beam characteristics [12] confirmed that each ring carries approximately the same energy and that these beams have planar fronts with π-phase shift from one Bessel ring to the next. Beam width definitions based on the second-order of irradiance in polar coordinates have been used to calculate the beam propagation factor – M^2 of nondiffracting beams and the resulting large values apparently contradict the nondiffracting character [13, 14]. Therefore, alternative methods of characterization, relying on the one-dimensional character of Bessel-type nondiffractive beams and on the fact that the useful part of these beams is often limited to their near-field, are needed. The former of these features leads to decomposition of a cylindrically symmetric resulting beam in rectangularly symmetric constituent beams describing the conical structure of resulting beam [15–17]. It is irradiance of the resulting beam from the spatial frequency domain, that is from the far-field, which is decomposed into angular sections corresponding to constituent waves. We propose a description of the Bessel beam in the propagation range, that is in the near-field, by using the so called self-convergent width [18], a method which has been used to characterize propagation of beams diffracted by hard-edge apertures. We show that this method can be used to characterize propagation invariant behavior of nondiffracting Bessel beams. The method is outlined in Section 2, Section 3 presents experimental generation of nondifracting Bessel beams, Section 4 describes the results of propagation measurements, and Section 5 concludes the paper.

2. SELF-CONVERGENT BEAM WIDTH

We first recall self-convergent beam width definition [18]. Beam width W, defined with the second-order moment of the beam irradiance, $I(x, z)$, can be written as

$$W = 2\sigma ,\qquad(1)$$

where

$$\sigma^2 = \frac{1}{P}\int_{-x_{\lim}}^{x_{\lim}} I(x,z)x^2\,\mathrm{d}x ,\qquad(2)$$

is the second-order moment (σ denotes the standard deviation), P, defined as

$$P = \int_{-x_{\lim}}^{x_{\lim}} I(x,z)\,\mathrm{d}x ,\qquad(3)$$

is the total power,

and $x_{\lim} \to \infty$. By integrating over a finite domain (instead of an infinite one) one obtains the so-called truncated second-order moment and the corresponding beam width.

A specific finite value for $x_{\lim}$ can be chosen according to the self-convergent-width truncation criterion. According to this criterion, the value of the integration limit that has to be used in Eqs. (2) and (3) is given by

$$x_{\lim} = F_s W(F_s),\tag{4}$$

where $W(F_s)$ is the self-convergent width and F_s is a positive constant called the self-convergent-width factor. The self-convergent width can be found through the following iterative procedure. First, an arbitrary initial value of the beam width is chosen, then the next value of the beam width is calculated with Eqs. (1) and (2), with the initial beam-width value multiplied by an arbitrary value chosen for the factor F_s used as the integration limit. The value of the beam width just obtained, multiplied again by the same factor F_s, is taken as the new integration limit for calculating the next value of the beam width. This procedure is repeated until the result remains practically unchanged, and the corresponding beam-width value is called the self-convergent width. This beam width depends on the factor F_s but not on the initial value of the beam width.

3. GENERATION OF NONDIFFRACTIVE BEAMS

For the generation of nondifractive Bessel beams we used an axicon displayed on a liquid crystal spatial light modulator (LC-SLM) in off-axis Fresnel configuration [19]. This configuration, in which the Bessel beam starts immediately after the plane of the SLM, allows better utilization of incident light as compared with the scheme using annular aperture [1]. The optical setup is shown in Fig. 1. A He-Ne laser (HRP020, Thorlabs) with a wavelength $\lambda = 633$ nm and linear polarization was used as light source. A half wavelength plate (HWP) was used to ensure that light polarization direction is aligned with LC molecules' orientation. The laser beam, that was spatially filtered with the lens L_1 ($f_1 = 16$ mm) and the microaperture P (diameter 25 micron) and collimated with lens L_2 ($f_2 = 150$mm), was then directed with the plane mirrors M_1 and M_2 toward the phase-only SLM with 1920×1080 pixel of 8×8 μm^2 (Pluto NIR2, Holoeye) at an incidence angle of about 3º. The 1st order of the diffracted light was incident on the lens L_4 ($f_4 = 300$ mm) which forms a telescope together with lens L_3 ($f_3 = 620$ mm) that was displayed on the SLM. Light was detected with the charge coupled device camera (CCD) of a beam analyzer (LBA-USB230, Spiricon). A variable neutral density filter (NDF) was inserted to exploit as much as possible of the CCD dynamic range. The CCD was mounted on a rail in order to measure beam propagation.
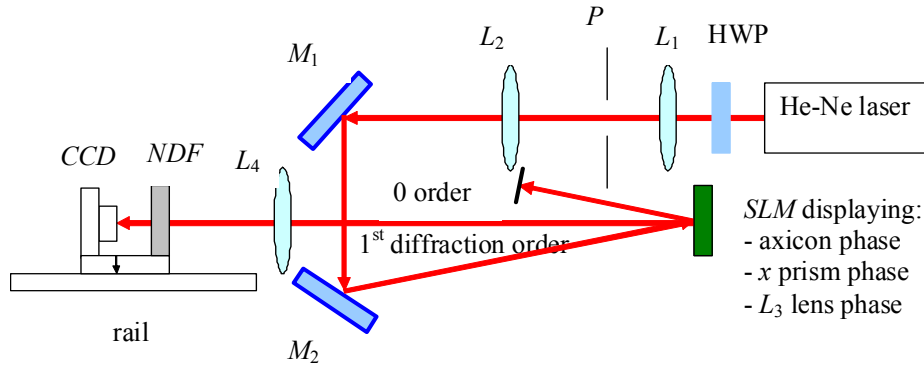
Fig. 1 – Optical setup for generation of nondiffracting beams.

The SLM was calibrated with the PhaseCam software [20] to have a phase delay that varies linearly with the applied voltage, on a 2π range. The phase displayed by the SLM contained three terms: (i) axicon phase, (ii) lens L_3 phase and (iii) linear prism phase to maximize 1st order diffraction efficiency. The zeroth diffraction order was blocked.

4. MEASUREMENT OF NONDIFFRACTIVE BEAMS PROPAGATION

Nondiffractive beams propagation has been analyzed by measuring transverse irradiance distribution at different planes $z =$ constant along the propagation axis. A typical profile of the beam irradiance, $I(x,y)$, taken at 0.79 m from lens L_4 for an axicon deflecting at $\theta_{axicon} = 1.31$ mrad, is presented in Fig. 2.
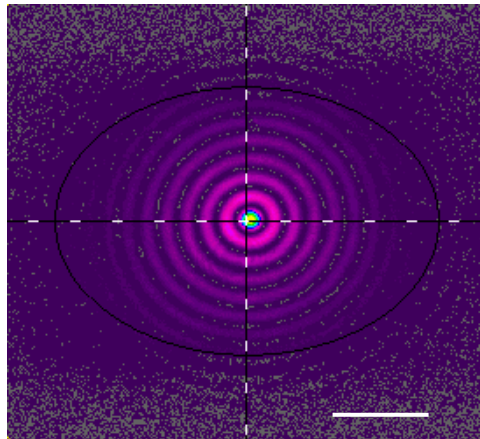

Fig. 2 – Typical Bessel beam irradiance profile measured for an axicon deflecting at $\theta = 1.31$ mrad. Irradiance is taken at 0.79 m from lens L_4. White bar length is 1 mm.

The pronounced peak surrounded by rings, two features specific to the Bessel beam profile, can be observed. In order to estimate the geometric focal range for the Bessel beam, Z_{max}, the peak irradiance, $I_{peak}(z) = I(0, 0, z)$ was measured as a function of z and the result is presented in Fig. 3. When the peak irradiance decreases below half of its maximum value the irradiance profile changes significantly from a Bessel beam profile. The value estimated for Z_{max} is about 0.35 m.
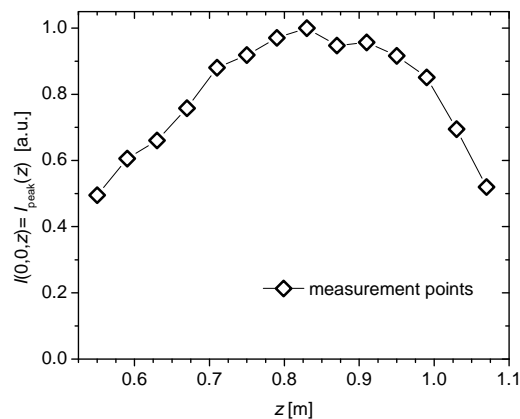

Fig. 3 – Peak irradiance $I_{peak}(z) = I(0, 0, z)$ as a function of distance z from lens L_4.
The maximum value is used for normalization.

The propagation of the profile $I(x, 0, z)$ at $z = 0.55$, 0.67 and 0.79 m from lens L_4 is presented in Fig. 4, where the maximum value of irradiance is used for normalization.
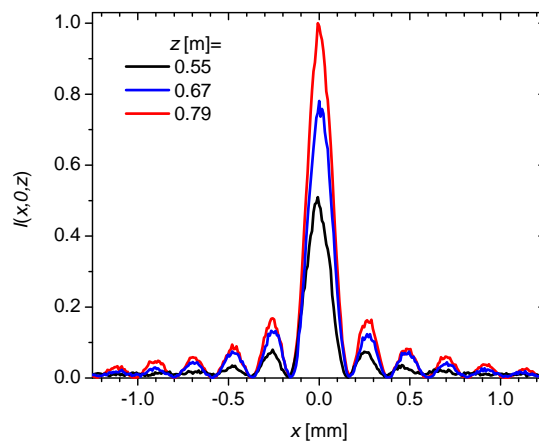

Fig. 4 – Cross section $I(x, 0, z)$ at $z = 0.55$, 0.67 and 0.79 m from lens L_4.
The maximum value of irradiance is used for normalization of the profiles.

The function

$$I(x) = A J_0^2\big(k_x(x - x_0)\big) + B \tag{5}$$

was fitted to the profile taken at the plane where peak irradiance has its maximum value and the result is shown in Fig. 5, where the experimental result is represented with the black line and the fitted function with the gray line.
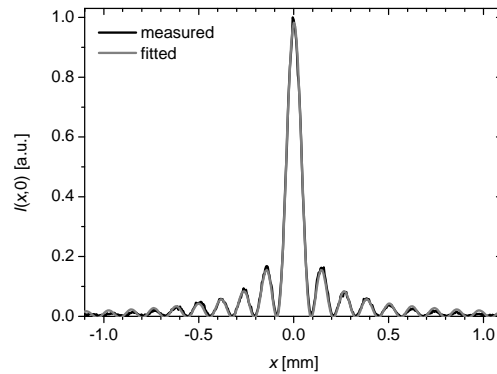

Fig. 5 – Cross section of beam irradiance profile $I(x, 0)$ at taken at the plane where peak irradiance has its maximum value. Measurement result is represented with the black line and fitted function with the gray line.

The values determined for the fitting parameters are $A = 0.99$ (a.u.), $B = -0.004$ (a.u.), $x_0 = 0.001$ mm and $k_x = 26.5$/mm. The value of the half angle θ of the cone around propagation axis on which the wave vectors of plane waves set lie, calculated with $\theta \approx \tan\theta = k_x\lambda/(2\pi)$, is 2.67 mrad. This value agrees with the corresponding design value for the axicon displayed on the SLM $(f_3/f_4)\theta_{\text{axicon}} = 2.71$.

The self-convergent width was calculated with Eqs. (1–4) and the result obtained for a self-convergent-width factor $F_s = 1.97$ is shown in Fig. 6.
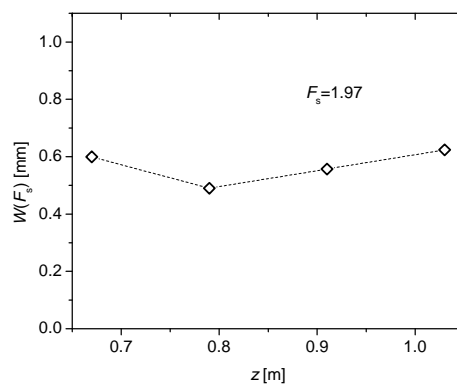

Fig. 6 – Self-convergent width, $W(F_s)$, calculated for $F_s = 1.97$, as a function of propagation distance.

Within a measurement error of about 25–30%, the self-convergent width propagation confirms the nondiffractive propagation of Bessel beam.

5. CONCLUSIONS

Self-convergent truncation criterion has been used to calculate the second-order beam width of nondiffractive Bessel beams in their propagation range. Within the measurement error, self-convergent beam width propagation confirms propagation invariant beahavior of these beams. Self-convergent beam width could be useful to characterize propagation of other nondiffractive beams.

REFERENCES

1. J. Durnin, J. Miceli Jr. and J. H. Eberly, Phys. Rev. Lett., **58**, 1499–1501 (1987).
2. J. Durnin, J. Opt. Soc. Am. A, **4**, 651–654 (1987).
3. F. Gori, G. Guattari and C. Padovani, Optics Commun., **64**, 491–495 (1987).
4. M. Padgett, Nat. Photonics, **4**, 741–742 (2010).
5. F. O. Fahrbach, P. Simon and A. Rohrbach, Nat. Photonics, **4**, 780–785 (2010).
6. V. Garces-Chavez, D. McGloin, H. Melville, W. Sibbett, K. Dholakia, Nature, **419**, 145–147 (2002).
7. M. Duocastella, C. B. Arnold, Laser Photonics Rev., **6**, 607–621 (2012).
8. C. Z. Cil, H. T. Eyyuboglu, Y. Baykal, O. Korotkova, Appl Phys B, **98**, 195–202 (2010).
9. P. Sprangle, B. Hafizi, Phys. Rev. Lett., **66**, 837 (1987).
10. R. P. MacDonald, S. A. Boothroyd, T. Okamoto, J. Chrostowski, B. A. Syrett, Optics Commun., **122**, 169–177 (1996).
11. Z. Bouchal, J. Wagner, M. Chlup, Optics Commun., **151**, 207–211 (1998).
12. Y. Lin, W. Seka, J. H. Eberly, H. Huang, and D. L. Brown, Appl. Opt., **31**, 2708–2713 (1992).
13. R. Borghi, M. Santarsiero, Opt. Lett., **22**, 262–264 (1997).
14. R. M. Herman, T. A. Wiggins, Appl. Opt., **37**, 3398–3400 (1998).
15. G. Rousseau, D. Gay and M. Piche, J. Opt. Soc. Am. A, **22**, 1274–1287 (2005).
16. G. Rousseau, D. Gay and M. Piche, Opt. Exp., **13**, 7589–7598 (2005).
17. G. Rousseau, D. Gay and M. Piche, Optics Commun., **265**, 261–269 (2006).
18. S. Amarande, A. Giesen and H. Hügel, Appl. Opt., **39**, 3914–3924 (2000).
19. A. Jesacher, S. Fürhapter, S. Bernet and M. Ritsch-Marte, Opt. Express, **12**, 2243–2250 (2004).
20. http://www.holoeye.com